THE GEOLOGICAL SOCIETY OF AMERICA®

The M_w 8.3 Illapel earthquake (Chile): Preseismic and postseismic activity associated with hydrated slab structures

Piero Poli[1], Andrei Maksymowicz Jeria[2], and Sergio Ruiz[2]
[1]Department of Earth, Atmospheric, and Planetary Sciences, Massachusetts Institute of Technology, Cambridge, Massachusetts 02139, USA
[2]Departamento de Geofísica, Facultad de Ciencias Físicas y Matemáticas, Universidad de Chile, Santiago, Chile

ABSTRACT

The accumulated stress in subduction zones is discharged with earthquake and aseismic activity; the latter is hosted in rheological complex regions, characterized by high pore fluid pressure, and is often accompanied by repeated earthquakes and earthquake swarms. The spatiotemporal analysis of seismic activity can reveal the presence of aseismic transients associated with large earthquakes. Here we study 20 years of seismicity prior to and after the M_w 8.3 earthquake that occurred in A.D. 2015 in central Chile. We identified several earthquake swarms before the main shock and repeating aftershocks at the border of the main slip area. Spatial clustering of the seismic activity shares similar orientation with the main fracture zones observed on the outer rise of the subducting Nazca plate. Our findings suggest that the fracture zones enclosing the rupture are playing a major role in accommodating the pre and post–main shock stress evolution. We further recognize how fracture regions have acted as barriers to the propagation of large earthquakes in the region.

INTRODUCTION

On 16 September 2015, a M_w 8.3 earthquake struck the north-central Chile subduction zone near the city of Illapel. This event broke a 150 × 100 km area (Melgar et al., 2016; Tilmann et al., 2016; Ruiz et al., 2016), and terminated to the north and to the south at two low interseismic coupling zones (Ruiz et al., 2016; Métois et al., 2016). In a similar manner, earthquakes in 1943 and 1880 could have stopped in the same zones (Beck et al., 1998). The northern rupture limit of the Illapel event coincides with the Challenger Fracture Zone and La Serena low interseismic coupling zone (Métois et al., 2016); the northern termination of the 1730 megaearthquake (M_w ~ 9.0) (Ruiz et al., 2016) and the southern extent of the 1922 Atacama megaearthquake also coincide with these features. The southern limit of the 2015 Illapel earthquake is close to the Juan Fernández ridge and the low interseismic coupling zone offshore Los Vilos at 31.8°S (Métois et al., 2016). Series of historical earthquakes (i.e., 1822, 1906, and 1971; Ruiz et al., 2016) show a northern extent of rupture at this latitude. Persistent seismicity has been observed in the past 20 yr around the Illapel region, with several swarm activities near the fracture zones, together with seismicity migration, aseismic slip (Gardi et al., 2006), and the occurrence of intraslab events such as the M_w 7.1 Punitaqui earthquake in 1997 (Lemoine et al., 2001; Pardo et al., 2002; Holtkamp et al., 2011) (Fig. 1; Figs. DR1 and DR2 in the GSA Data Repository[1]).

[1]GSA Data Repository item 2017064, identification of repeating earthquakes, and Figures DR1–DR5, is available online at http://www.geosociety.org/datarepository/2017 or on request from editing@geosociety.org.

The regions around the main slip area of the Illapel earthquake also host large afterslip (Barnhart et al., 2016).

Little sedimentary fill of the trench and the high convergence rate of 6.8 cm/yr (Vigny et al., 2009) favor the process of tectonic erosion (Clift and Vannucchi, 2004) in the Illapel region. The roughness of the slab, resulting from tectonic evolution of the oceanic plate before its subduction, generates high fracturing in the interplate boundary and favors the collapse of the continental wedge due to the process of basal tectonic erosion (Contreras-Reyes et al., 2015). Therefore, the long-term rheological conditions at the interplate boundary are related to heterogeneities, both in the oceanic and continental crust. Numerous papers have highlighted the relation between subducted features and the earthquake sources; one example of this is the location of asperities around subducted seamounts (Cloos, 1992; Bilek et al., 2003). However, the process of seamount subduction can also prevent slips under favorable conditions of fluid migration and fracturing (Mochizuki et al., 2008; Wang and Bilek, 2014). Moreover, a correlation of the subducted aseismic ridges and fracture zones with the distribution of earthquakes is observed along the subduction margins (Kelleher and McCann, 1976; Contreras-Reyes and Carrizo, 2011; Nishikawa and Ide, 2015). However, observation of high pore-fluid pressure is also correlated with low interseismic locking regions (Moreno et al., 2014). These hydrated regions are also the locus of aseismic phenomena as slow slips and earthquake swarms (Rogers and Dragert, 2003; Saffer and Wallace, 2015, and references therein).

We analyzed geological and seismological data, which suggest a complex distribution of frictional properties on the megathrust in the Illapel area. Our study also suggests the presence of aseismic slip in the hydrated regions, taking place for at least 20 yr before the event. The same regions are hosting large postseismic slip.

TECTONIC SETTING

The northern limit of the Illapel coseismic slip patch correlates with the subducted trace of the Challenger Fracture Zone at ~30°S (Fig. 1A). This large structure corresponds to a northward slab age discontinuity of ~5 m.y. (Müller et al., 2008), but it is not associated with high roughness in the seafloor, suggesting little or no disruptive effect on the margin. The total magnetic intensity anomaly reveals a width of 40 km for this structure and the free-air gravity anomaly shows local subsidence of the continental wedge aligned with its trace (Fig. DR3), which we interpreted as an effect of high fluid content on the interplate boundary along the Challenger Fracture Zone that reduces the effective basal friction coefficient, generating a local bathymetry low with the corresponding decrease of slope angle (Maksymowicz, 2015).

Observing the swath bathymetric data of the studied area (Contreras-Reyes et al., 2015), we identified and traced large structures formed by the Nazca plate bending (black lines in Fig. 1A) that show a rotation from a northeast strike south of ~31°S to a near north-south direction to the north. The oblique-strike structures are located around the Juan Fernández ridge, suggesting that its collision with the subduction margin (joined with its buoyancy) locally rotates the stress field. According to the bathymetry the influence of the Juan Fernández ridge on the oceanic fracturing is extended to 100 km around the ridge trace. A conjugate set of outer-rise structures is observed with northwest direction (some of these structures are shown with red lines in Fig. 1A) with a strike similar to that observed for the magnetic fabric of the slab (magenta lines in Fig. 1A). We interpret this second structural set as fractures generated at the spreading center that are possibly reactivated near the trench (similar to Ranero et al., 2005). Ranero et al. (2005) showed evidence

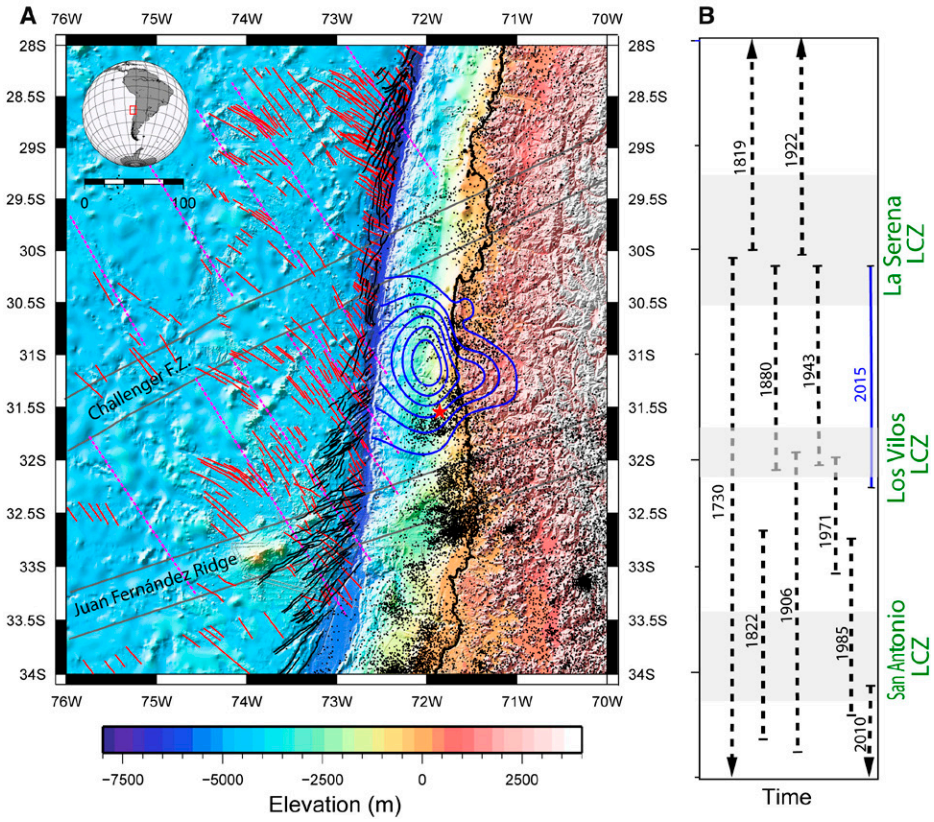

Figure 1. The seismotectonic setting of the Illapel (Chile) earthquake region. A: The oceanic Nazca plate structures and the Chilean National Seismological Center (CSN) catalog seismicity (black dots) are presented over a satellite-swath bathymetry elevation model. Magenta lines indicate the directions of the magnetic fabric in the Nazca plate. Red lines highlight the structures generated at the spreading center during the slab formation, and black lines show the outer-rise faulting observed in the swath bathymetry. The red star is the epicenter of the Illapel earthquake, and blue curves correspond to the slip contours (each 1 m) of the Illapel earthquake according to Ruiz et al. (2016). Gray lines highlight the traces of the Challenger Fracture Zone (F.Z.) and Juan Fernández ridge. B: Rupture lengths of historic earthquakes. Gray hachured areas are low coupling zones from Métois et al. (2016). LCZ—low interseismic coupling zone.

that some of these structures can be reactivated as intermediate-depth intraslab seismicity, highlighting a long-term permanence of the outer-rise faulting during the subduction process. The role of the slab faults in the interplate boundary is poorly understood, although the nature of these faults as important fluid transport zones has been observed seaward from the trench by numerous geophysical studies, such as reflection seismic experiments (Ranero et al., 2003; Han et al., 2016), electromagnetic surveys (Naif et al., 2015), and wide-angle seismic tomography that show a decrease of Vp and Vs (P and S wave velocities) inside the oceanic crust and mantle, which are interpreted as an effect of the hydration process favored by the fault bending (Contreras-Reyes et al., 2008; Moscoso and Grevemeyer, 2015; Shillington et al., 2015). It is important to note that the extension of the outer-rise fault lengths at the sea bottom is typically >50 km, indicating their crustal-scale influence and that they probably reach the upper mantle below an ~7-km-thick oceanic crust (Zelt et al., 2003).

SEISMICITY ANALYSIS

For a detailed study of the seismicity in the Illapel region, we compiled a composite catalog. We use the U.S. Geological Survey National Earthquake Information Center catalog from 1990 to 2000, and for data since 2000, the Chilean National Seismological Center (CSN) catalog. Our composedcatalog has a time-variable completeness around magnitude 4.0. The observed seismicity shows a pattern complementary to the slip distribution of the Illapel M_w 8.3 earthquake (Fig. 2A; Fig. DR1). Most of the events are located near the north, south, and east edges of the 2015 Illapel asperity. A similar pattern is recognized in the aftershock distribution (Tilmann et al., 2016; Figs. DR1 and DR2) and postseismic slip (Barnhart et al., 2016).

Several swarms can be observed in the time-dependent seismicity plot (Fig. 2B; Figs. DR1 and DR2). We consider a swarm as a cluster of events in time, space, and magnitude (Holtkamp et al., 2011). The most remarkable swarm started in July 1997 and ended in February 1998 (Gardi et al., 2006, Holtkamp et al., 2011). The swarm started in zone 1, then a stress transfer from the aseismic slip at depths >50 km triggered the swarm of zone 2 and the Punitaqui 1997 M_w 7.1 intraslab earthquake (Gardi et al., 2006). Zone 3 is characterized by a sudden change of seismicity rates after the Punitaqui swarm in 1997 (Fig. 2B). Zones 1 and 2 underwent seismicity acceleration from February to June 2003 (Fig. 2B). Seismicity starts in zone 1, with interplate events at depth <30 km, and extends downdip (depth >30 km) in zone 2. Since 2005, we only observed swarms in zone 3, including a small swarm that happened some weeks before the main shock in Illapel (Figs. DR1K and DR2K).

We also found 86 repeating earthquakes (Fig. 2A; see the Data Repository), 3 of which occurred before the main shock (Fig. 2C). The magnitude of the repeating events spanned M_w 4–M_w 4.9and they were localized in the same place of the observed swarms (zones 1, 2, and 3) where large afterslip is occurring (Barnhart et al., 2016).

The spatial distribution of the repeaters and normal seismicity follow a preferential north-south distribution on zone 1 (Fig. 2) and a WSW–ENE alignment in zone 3 (Fig. 2). This feature correlates with the strike of bending slab fractures seaward to the trench (Fig. 1A).

DISCUSSION

The ensemble of our observations is shown in Figure 3. The geological interpretation of the magnetic intensity anomaly, the free-air gravity anomaly, and the swath bathymetric data revealed important fractured zones in the Nazca plate. The signature of the fractures is likely to extend to the seismogenic zone contact. The orientation of slab faults correlates with the preferential orientation of earthquake swarms and repeaters. We can thus define two or three main fractured zones in the seismogenic contact that are most relevant. These fracture zones control the seismicity of zones 1, 2, and 3 (Fig. 3). Despite the lack of three-dimensional velocity models in the zone that show low values of Vp and Vs, we propose that zones 1, 2, and 3 have high pore-fluid pressure favoring the presence of persistent swarm-type seismicity (Fig. 2). The correlation of the fracture zones with the observed low interseismic coupling value (Ruiz et al., 2016; Métois et al., 2016) supports our hypothesis and suggests the important role of water in controlling the frictional behavior of the plate interface, as proposed in Moreno et al. (2014). Why some of the subducted slab fractures favored the seismic activity, rather than others, cannot be explained without a complete knowledge of the stress and strain fields on the interplate boundary. However, it is a common behavior of the seismogenic zones that only few structures of the complete set of faults are seismically active at the same time, depending on the stress field and the rheology of the faults.

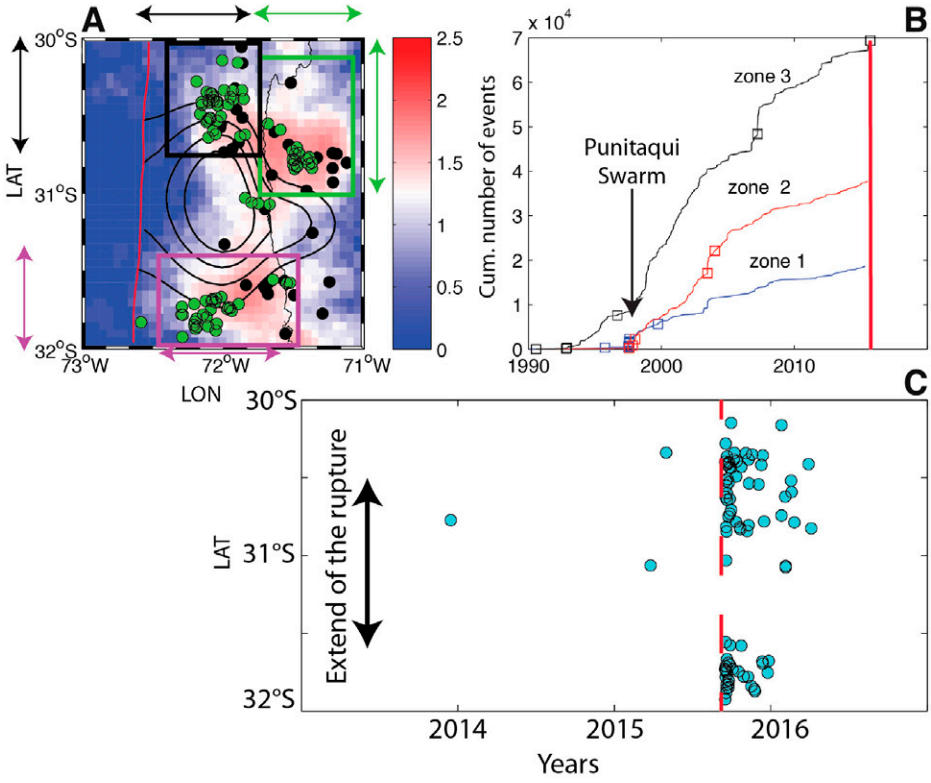

Figure 2. A: Seismicity in the Illapel area (Chile). The color map represents the logarithmic summation of the seismicity in a 0.1° grid from A.D. 1990 to the time of the Illapel earthquake. The 1 m contour of the 2015 Illapel coseismic slip is plotted as black lines. Black dots are events of moment magnitude, M_w, >5.5. Green dots are the 86 repeating earthquakes. We identified three zones (outlined boxes) where most seismicity and repeaters are located. Red line is the trench B: Time-dependent cumulative (Cum.) seismicity for zone 1 (31°S–30°S, 72.5°W–71.8°W, black box in A), zone 2 (31°S–30°S, 71.8°W–71°W, green box in A), and zone 3 (32°S–31.2°S, 72.5°W–71.5°W, violet box in A). The squares are events with M_w > 5.5. Red line is the time of the Illapel earthquake C: Repeating events (blue dots) plotted as function of latitude (approximately along trench) and occurrence time. The red vertical dashed line is the time of the Illapel earthquake.

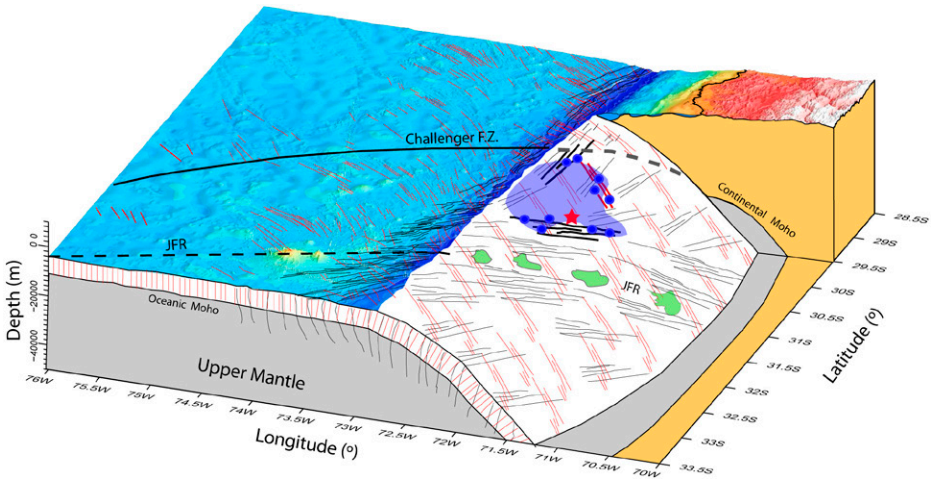

Figure 3. Conceptual model for the hydrated structures and seismicity at the interplate boundary. The figure presents a hypothetical view from the southeast. The red star is the epicenter of the Illapel (Chile) earthquake, blue circles exemplify repeating and swarm, and the blue area represents the associated rupture zone. On the subducted slab, the red lines are the structures generated during the slab formation, and black lines show the faults generated at the outer-rise zone. According to the model, some of these structures (bold lines) release fluids to the contact, favoring the generation of swarms and repeaters. In particular, the Illapel earthquake was stopped to the south by some of these hydrated structures, parallel to the Juan Fernández ridge (JFR) direction. F.Z.—fracture zone.

The fluid-rich low coupling regions act as barriers to propagation during large megathrust events (Figs. 1B and 3) and host high seismicity rates in the interseismic and postseismic periods (Sammonds et al., 1992; Schlaphorst et al., 2016). The swarm-like seismicity and repeating earthquakes are characteristic of fluid-rich and geologically complex regions (Fagereng and Sibson, 2010) and are associated with slow slip events (Crescentini et al., 1999; Rogers and Dragert, 2003; Saffer and Wallace, 2015, and references therein) and postseismic deformation (Nadeau and Johnson, 1998; Perfettini et al., 2010). We thus have enough evidence to recognize the presence of aseismic slip at the border of the Illapel asperity at least since 1997, together with a large afterslip (Barnhart et al., 2016).

The overall seismic behavior of the plate interface in the Illapel region seems to obey the rate and state formalism shown by numerical simulation (Kaneko et al., 2010), with a high seismicity rate near the low coupling region and a moderate seismic rate inside the locked zones. From our analysis, we can conclude the important role of hydrated geological features in controlling the megathrust coupling and in modulating the stress. Our study illustrates the importance of integrated geological and seismological data analysis to inform predictive models for long-term megathrust dynamics.

ACKNOWLEDGMENTS

Maksymowicz Jeria and Ruiz were supported by La Comisión Nacional de Investigación Científica y Tecnológica (CNICYT) of Chile projects FONDECYT 3150160 and 11130230. Poli acknowledges U.S. National Science Foundation grant EAR-1521534. We thank the Centro Sismológico Nacional (CSN; Chile) for making the data available to us.

REFERENCES CITED

Barnhart, W.D., Murray, J.R., Briggs, R.W., Gomez, F., Gomez, C.P.J., Miles, J., Svarc, S., Riquelme, S., and Stressler, B.J., 2016, Co-seismic slip and early afterslip of the 2015 Illapel, Chile earthquake: Implications for frictional heterogeneity and coastal uplift: Journal of Geophysical Research, v. 121, p. 6172–6191, doi:10.1002/2016JB013124.

Beck, S., Barrientes, S., Kausel, E., and Reyes, M., 1998, Source characteristics of historic earthquakes along the central Chile subduction zone: Journal of South American Earth Sciences, v. 11, p. 115–129, doi:10.1016/S0895-9811(98)00005-4.

Bilek, S.L., Schwartz, S.Y., and DeShon, H., 2003, Control of seafloor roughness on earthquake rupture behavior: Geology, v. 31, p. 455–458, doi:10.1130/0091-7613(2003)031<0455:COSROE>2.0.CO;2.

Clift, P., and Vannucchi, P., 2004, Controls on tectonic accretion versus erosion in subduction zones: Implications for the origin and recycling of the continental crust: Reviews of Geophysics, v. 42, RG2001, doi:10.1029/2003RG000127.

Cloos, M., 1992, Thrust-type subduction-zone earthquakes and seamount asperities: A physical model for seismic rupture: Geology, v. 20, p. 601–604, doi:10.1130/0091-7613(1992)020<0601:TTSZEA>2.3.CO;2.

Contreras-Reyes, E., and Carrizo, D., 2011, Control of high oceanic features and subduction channel on earthquake ruptures along the Chile-Peru subduction zone: Physics of the Earth and Planetary Interiors, v. 186, p. 49–58, doi:10.1016/j.pepi.2011.03.002.

Contreras-Reyes, E., Grevemeyer, I., Flueh, E.R., Scherwath, M., and Bialas, J., 2008, Effect of trench-outer rise bending-related faulting on seismic Poisson's ratio and mantle anisotropy: A case study offshore of southern central Chile: Geophysical Journal International, v. 173, p. 142–156, doi:10.1111/j.1365-246X.2008.03716.x.

Contreras-Reyes, E., Ruiz, J., Becerra, J., Kopp, H., Reichert, C., Makysymowicz, A., and Arriagada, C., 2015, Structure and tectonics of the central Chilean margin (31°–33°S): Implications for subduction erosion and shallow crustal seismicity: Geophysical Journal International, v. 203, p. 776–791, doi:10.1093/gji/ggv309.

Crescentini, L., Amoruso, A., and Scarpa, R., 1999, Constraints on slow earthquake dynamics from a swarm in central Italy: Science, v. 286, p. 2132–2134, doi:10.1126/science.286.5447.2132.

Fagereng, A., and Sibson, R.H., 2010, Melange rheology and seismic style: Geology, v. 38, p. 751–754, doi:10.1130/G30868.1.

Gardi, A., Lemoine, A., Madariaga, R., and Campos, J., 2006, Modeling of stress transfer in the Coquimbo region of central Chile: Journal of Geophysical Research, v. 111, B04307, doi:10.1029/2004JB003440.

Han, S., Carbotte, S.M., Canales, J.P., Nedimović, M.R., Carton, H., Gibson, J.C., and Horning, G.W., 2016, Seismic reflection imaging of the Juan de Fuca plate from ridge to trench: New constraints on the distribution of faulting and evolution of the crust prior to subduction: Journal of Geophysical Research, v. 121, p. 1849–1872, doi:10.1002/2015JB012416.

Holtkamp, S.G., Pritchard, M.E., and Lohman, R.B., 2011, Earthquake swarms in South America: Geophysical Journal International, v. 187, p. 128–146, doi:10.1111/j.1365-246X.2011.05137.x.

Kaneko, Y., Avouac, J.-P., and Lapusta, N., 2010, Towards inferring earthquake patterns from geodetic observations of interseismic coupling: Nature Geoscience, v. 3, p. 363–369, doi:10.1038/ngeo843.

Kelleher, J., and McCann, W., 1976, Buoyant zones, great earthquakes, and unstable boundaries of subduction: Journal of Geophysical Research, v. 81, p. 4885–4896, doi:10.1029/JB081i026p04885.

Lemoine, A., Campos, J., and Madariaga, R., 2001, Evidence for earthquake interaction in the Illapel Gap of central Chile: Geophysical Research Letters, v. 28, p. 2743–2746, doi:10.1029/2000GL012314.

Maksymowicz, A., 2015, The geometry of the Chilean continental wedge: Tectonic segmentation of subduction processes off Chile: Tectonophysics, v. 65, p. 183–196, doi:10.1016/j.tecto.2015.08.007.

Melgar, D., Fan, W.Y., Riquelme, S., Geng, J.H., Liang, C.R., Fuentes, M., Vargas, G., Allen, R.M., Shearer, P.M., and Fielding, E.J., 2016, Slip segmentation and slow rupture to the trench during the 2015, Mw 8.3 Illapel, Chile earthquake: Geophysical Research Letters, v. 43, p. 961–966, doi:10.1002/2015GL067369.

Métois, M., Vigny, C., and Socquet, A., 2016, Interseismic coupling, megathrust earthquakes and seismic swarms along the Chilean Subduction Zone (38°–18°S): Pure and Applied Geophysics, v. 173, p. 1431–1449, doi:10.1007/s00024-016-1280-5.

Mochizuki, K., Yamada, T., Shinohara, M., Yamanaka, Y., and Kanazawa, T., 2008, Weak interplate coupling by seamounts and repeating M > 7 earthquakes: Science, v. 321, p. 1194–1197, doi:10.1126/science.1160250.

Moreno, M., Haberland, C., Oncken, O., Rietbrock, A., Angiboust, S., and Heidach, O., 2014, Locking of the Chile subduction zone controlled by fluid pressure before the 2010 earthquake: Nature Geoscience, v. 7, p. 292–296, doi:10.1038/ngeo2102.

Moscoso, E., and Grevemeyer, I., 2015, Bending-related faulting of the incoming oceanic plate and its effect on lithospheric hydration and seismicity: A passive and active seismological study offshore Maule: Chile Journal of Geodynamics, v. 90, p. 58–70, doi:10.1016/j.jog.2015.06.007.

Müller, R.D., Sdrolias, M., Gaina, C., and Roest, W.R., 2008, Age, spreading rates, and spreading asymmetry of the world's ocean crust: Geochemistry, Geophysics, Geosystems, v. 9, Q04006, doi:10.1029/2007GC001743.

Nadeau, R.M., and Johnson, L.R., 1998, Seismological studies at Parkfield VI: Moment release rates and estimates of source parameters for small repeating earthquakes: Seismological Society of America Bulletin, v. 88, p. 790–814.

Naif, S., Key, K., Constable, S., and Evans, R.L., 2015, Water-rich bending faults at the Middle America Trench: Geochemistry, Geophysics, Geosystems, v. 16, p. 2582–2597, doi:10.1002/2015GC005927.

Nishikawa, T., and Ide, S., 2015, Background seismicity rate at subduction zones linked to slab-bending-related hydration: Geophysical Research Letters, v. 42, p. 7081–7089, doi:10.1002/2015GL064578.

Pardo, M., Comte, D., Monfret, T., Boroschek, R., and Astroza, M., 2002, The October 15, 1997 Punitaqui earthquake (Mw=7.1): A destructive event within the subducting Nazca plate in central Chile: Tectonophysics, v. 345, p. 199–210, doi:10.1016/S0040-1951(01)00213-X.

Perfettini, H., et al., 2010, Seismic and aseismic slip on the Central Peru megathrust: Nature, v. 465, p. 78–81, doi:10.1038/nature09062.

Ranero, C.R., Morgan, J.P., McIntosh, K., and Reichert, C., 2003, Bending-related faulting and mantle serpentinization at the Middle America trench: Nature, v. 425, p. 367–373, doi:10.1038/nature01961.

Ranero, C.R., Villaseñor, A., Phipps Morgan, J., and Weinrebe, W., 2005, Relationship between bend-faulting at trenches and intermediate-depth seismicity: Geochemistry, Geophysics, Geosystems, v. 6, Q12002, doi:10.1029/2005GC000997.

Rogers, G., and Dragert, H., 2003, Episodic tremor and slip: The chatter of slow earthquakes: Science, v. 300, p. 1943–1944, doi:10.1126/science.1084783.

Ruiz, S., et al., 2016, The seismic sequence of the 16 September 2015 Mw 8.3 Illapel, Chile, Earthquake: Seismological Research Letters, v. 87, doi:10.1785/0220150281.

Saffer, D., and Wallace, L., 2015, The frictional, hydrologic, metamorphic and thermal habitat of shallow slow earthquakes: Nature Geoscience, v. 8, p. 594–600, doi:10.1038/ngeo2490.

Sammonds, P.R., Meredith, P.G., and Main, I.G., 1992, Role of pore fluids in the generation of seismic precursors to shear fracture: Nature, v. 359, p. 228–230, doi:10.1038/359228a0.

Schlaphorst, D., Kendall, J., Collier, J., Verdon, J., Blundy, J., Baptie, B., Latchman, J., Massin, F., and Bouin, M.P., 2016, Water, oceanic fracture zones and the lubrication of subducting plate boundaries—Insights from seismicity: Geophysical Journal International, v. 204, p. 1405–1420, doi:10.1093/gji/ggv509.

Shillington, D.J., Bécel, A., Nedimović, M.N., Kuehn, H., Webb, S.C., Abers, G.A., Keranen, K.M., Li, J., Delescluse, M., and Mattei-Salicrup, G.A., 2015, Link between plate fabric, hydration and subduction zone seismicity in Alaska: Nature Geoscience, v. 8, p. 961–964, doi:10.1038/ngeo2586.

Tilmann, F., et al., 2016, The 2015 Illapel earthquake, central Chile: A type case for a characteristic earthquake?: Geophysical Research Letters, v. 43, p. 574–583, doi:10.1002/2015GL066963.

Vigny, C., Rudloff, A., Ruegg, J.C., Madariaga, R., Campos, J., and Alvarez, M., 2009, Upper plate deformation measured by GPS in the Coquimbo Gap, Chile: Physics of the Earth and Planetary Interiors, v. 175, p. 86–95, doi:10.1016/j.pepi.2008.02.013.

Wang, K., and Bilek, S.L., 2014, Fault creep caused by subduction of rough seafloor relief: Tectonophysics, v. 610, p. 1–24, doi:10.1016/j.tecto.2013.11.024.

Zelt, C.A., Sain, K., Naumenko, J.V., and Sawyer, D.S., 2003, Assessment of crustal velocity models using seismic refraction and reflection tomography: Geophysical Journal International, v. 153, p. 609–626, doi:10.1046/j.1365-246X.2003.01919.x.

Manuscript received 25 August 2016
Revised manuscript received 19 November 2016
Manuscript accepted 22 November 2016

Printed in USA